

# Synchronized Phasor Measurement in Protective Relays for Protection, Control, and Analysis of Electric Power Systems

Gabriel Benmouyal, E. O. Schweitzer, and A. Guzmán  
*Schweitzer Engineering Laboratories, Inc.*

Published in  
*Wide-Area Protection and Control Systems: A Collection of  
Technical Papers Representing Modern Solutions, 2017*

Previously presented at the  
8th International Conference on Developments in Power System Protection, April 2004,  
57th Annual Conference for Protective Relay Engineers, March 2004,  
57th Annual Georgia Tech Protective Relaying Conference, May 2003,  
and InterNational Electrical Testing Association Technical Conference, March 2003

Originally presented at the  
29th Annual Western Protective Relay Conference, October 2002

# SYNCHRONIZED PHASOR MEASUREMENT IN PROTECTIVE RELAYS FOR PROTECTION, CONTROL, AND ANALYSIS OF ELECTRIC POWER SYSTEMS

---

Gabriel Benmouyal  
Schweitzer Engineering Laboratories, Inc.  
Longueuil, PQ CANADA

E. O. Schweitzer, A. Guzmán  
Schweitzer Engineering Laboratories, Inc.  
Pullman, WA USA

## ABSTRACT

The advent of satellite-based time-keeping systems and advances in computer technology have made possible protective relay sampling synchronization within 1  $\mu$ s. These relays can now provide synchronized phasor measurements that eliminate the need to have different devices for protection, control, and electric power system analysis for system-wide applications and traditional protection applications. System-wide applications have different sampling and signal processing requirements than do traditional protection applications. These different requirements normally are addressed with different devices, one device for each specific function. This paper proposes combining the aforementioned applications in a single device with a flexible signal processing system. The addition of synchrophasor measurement in a protective relay results in increased power system reliability and provides easier disturbance analysis, protection, and control capabilities than do approaches with different information sources.

**Keywords:** frequency, protective relays, sampling, synchronized phasor measurement, time synchronization

## INTRODUCTION

There may be a historical parallel between fault locating and phasor measurements in digital relays. Two decades ago, stand-alone fault locators were seldom used. They were relatively expensive and were only used on the most critical and troublesome lines. Then, distance relays that included fault locating appeared and were quickly accepted. After a decade, it was impossible to imagine a distance relay without fault-locating capabilities.

For some time now, stand-alone synchronized phasor measuring devices have been available. They are not in widespread use, because they too are relatively expensive and find use only on critical systems. Now, a distance relay is available that includes synchronized phasor measurement capabilities. As these relays are becoming widely used, especially on extra high-voltage systems, the phasor-measurement function is proliferating. It is no longer necessary to justify a phasor measurement capability since it comes “for free” with the line protection.

Just as was the case with fault locating, we need to understand how phasor measurement works and what it can do for us. That is the purpose of this paper.

We will first carefully define phasors and synchronized phasors. An IEEE standard defines the absolute time reference for phasors as the start of the second. These points in time are known to within a microsecond when satellite clock receivers are available. The standard does not define phase for off-frequency quantities, such as a system operating at 59.8 Hz. This paper clearly defines absolute phase, even at off-nominal frequencies.

We examine phase as an indicator of the dynamic performance of a power system, as is well appreciated in the dynamic swing equations.

The paper is careful to recognize that phasors represent systems assumed to be in steady state. If a system is swinging, or when a fault occurs, there are electrical and mechanical transients, and we must be careful how we calculate magnitude and phase, and equally careful in how we use or interpret these quantities during transients. We will show a method that uses a three-cycle moving average and that implies phase measurement updates 20 times per second, or about every 50ms. This is fast enough to follow the electromechanical action of the system, and slow enough to filter out electrical-transient behavior.

We review several methods of sampling and processing signals, and show that the preferred way for phasor measurement is to first sample the signals using a sampling clock which is in absolute time synchrony. Each sample then is taken at a precisely known and absolute time. Phase is calculated from these samples. Magnitude is calculated after a resampling at a multiple of the actual system frequency using Fourier filters.

The relay now measures absolute phase, as well as voltage, current, power, and reactive power. The relay therefore is a transducer, too. This transducer measures the state variables and other protective relay-related information.

The above, plus advances in affordable, available, fast, dependable wide-area communications, make new approaches to system stability monitoring and control become practical. One might perceive a wide-area system where relays measure and communicate state variables to one or more processing elements, every tenth of a second, for example. The processing elements, in turn, assess the overall system state and exercise wide-area control and other decisions.

The 10-minute problem of state *estimation* is reduced to a 0.1 second exercise of state *measurement*! The advent and broad deployment of relays having phasor measurement capability is a grand opportunity for providers of state estimators to simplify their calculations, to obtain more accurate state estimates, much more rapidly, probably with smaller, more reliable computing systems.

Synchronized measurements also ease analysis of oscillographic records, because all records can be immediately compared.

The paper also describes two types of information output: unsolicited binary messages and solicited ASCII messages. The unsolicited messages are generated automatically at a specified rate and could be compared to a transducer output. The solicited messages provide “snapshots” at instants the user specifies.

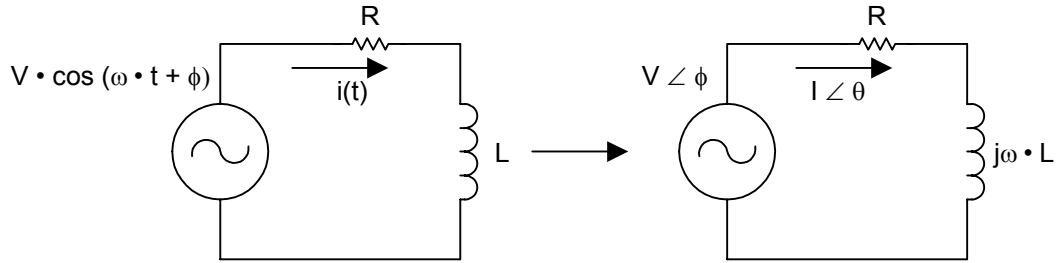
Finally, we mention the sources of error and conclude that accuracies of much less than one electrical degree are routinely achievable. The largest source of error is CCVT error.

Now that phasor measurement is becoming deployed “for free,” it will be fascinating to see the many creative applications that result and the many serious problems that are solved.

# VOLTAGE AND CURRENT TIME WAVEFORMS AND PHASOR DEFINITION

## The Origin of Phasors

Originally, phasors were introduced for the purpose of transforming electrical circuit differential equations into ordinary algebraic equations. As an example, consider the circuit of Figure 1.



a) Circuit in the time domain

b) Circuit in the frequency domain

**Figure 1** RL electrical circuit in the time and frequency domains

The solution of the following differential equation provides the solution for the circuit current:

$$V \cdot \cos(\omega \cdot t + \phi) = R \cdot i(t) + L \frac{di(t)}{dt} \quad (1)$$

The circuit being linear, the solution for the current has the following form:

$$i(t) = I \cdot \cos(\omega \cdot t + \theta) \quad (2)$$

We can represent voltage and current phasors as complex numbers in exponential form:

$$\bar{V} = V \cdot e^{j\phi} \text{ and } \bar{I} = I \cdot e^{j\theta} \quad (3)$$

The Appendix shows that we can express Equation 1 in algebraic form as follows:

$$V \cdot e^{j\phi} = (R + j\omega \cdot L) I \cdot e^{j\theta} \quad (4)$$

The solution for the current is:

$$I \cdot e^{j\theta} = \frac{V \cdot e^{j\phi}}{R + j\omega \cdot L} \quad (5)$$

From this example, we can infer the following:

1. A phasor is a complex number associated with a sinusoidal wave. The phasor magnitude is the same as the sinusoidal wave magnitude. The phasor phase angle is the phase of the wave at  $t = 0$ .
2. Phasors normally are associated with a single frequency.
3. To be able to remove the time dimension from the solution when applying the phasor transformation (see Appendix), all parameters in the system must be constant.

4. There is no need to define a time scale or a time reference in theoretical steady-state studies, because the time dimension has been removed from the final phasor-based equations (see Appendix).
5. In power network studies, application of phasors occurs in all problems where the parameters are constant and we have a single frequency. Load-flow or short-circuit programs are examples of such studies. For electromagnetic transient analysis, we usually solve the network differential equations in the time domain. Tools such as EMTP (Electromagnetic Transient Program) or the Power System Blockset [1] are examples of this approach. Theoretically in an actual power network, we could apply phasors only in steady-state conditions. As we will see later, we can still apply the phasor concept in transient conditions and obtain good results.

### **Definition of Synchronized Phasors**

The definition of a real-time or synchronized phasor provided in the IEEE Standard 1344-1995 [2] corresponds to the conventional definition described earlier, at least at rated frequency. Outside rated frequency, the standard opens the door for equipment manufacturers to develop their own definition (see Appendix C in Reference [2]); the standard has no requirement regarding phasor magnitude measurement accuracy outside system nominal frequency (50 Hz or 60 Hz).

With real-time waveforms, it is necessary to define a time reference to measure phase angles synchronously [3]. The IEEE Standard 1344-1995 [2] defines the start of the second as the time reference for establishing the phasor phase angle value. The synchronized phasor measurement convention is shown in Figure 2.

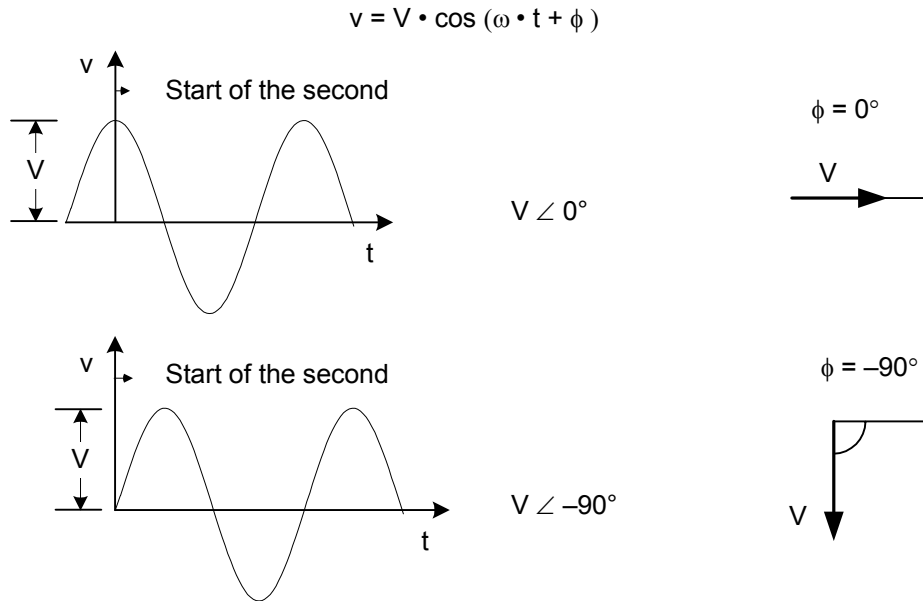


**Figure 2** Synchronphasor measurement convention with respect to time

The instantaneous phase angle measurement remains constant at rated frequency when using the start of the second phase reference. If the signal is at off-nominal frequency, the instantaneous phase varies with time. We shall see later that the choice of this reference has an impact on the phasor phase angle measurement at off-nominal frequency.

The IEEE Standard 1344-1995 [2] defines a steady-state waveform where the magnitude, frequency, and phase angle of the waveform do not change. This standard has no requirements regarding phasor measurement performance for a waveform in transient state.

### **Phase Measurement at Off-Nominal Frequencies**

Let the following function represent the voltage at a bus in a power system network:

$$V(t) = V \cdot \cos(2 \cdot \pi \cdot f \cdot t + \phi) \quad (6)$$

The argument of the cosine function in Equation 6 is:

$$\theta(t) = 2 \cdot \pi \cdot f \cdot t + \phi \quad (7)$$

At off-nominal frequencies, we can represent the argument,  $\theta$ , of the cosine function as follows:

$$\theta(t) = 2 \cdot \pi \cdot f_{\text{NOM}} \cdot t + 2 \cdot \pi \cdot \Delta f \cdot t + \phi \quad (8)$$

where:

$$\Delta f = f - f_{\text{NOM}}$$

If we subtract from  $\theta$  the angle measurement resulting from the nominal frequency,  $2 \cdot \pi \cdot f_{\text{NOM}} \cdot t$ , we obtain the angle measurement that includes the angle measurement caused by frequency deviation from nominal frequency,  $2 \cdot \pi \cdot \Delta f \cdot t$ , plus the phase angle at  $t = 0$ ,  $\phi$ . Following is the equation representing the new angle measurement:

$$\beta(t) = 2 \cdot \pi \cdot \Delta f \cdot t + \phi \quad (9)$$

At nominal frequency  $\Delta f = 0$ ,  $\beta(t) = \phi$ . At off-nominal frequency,  $\beta$  will change with time. Figure 3 shows  $\beta$  for  $\Delta f > 0$ .

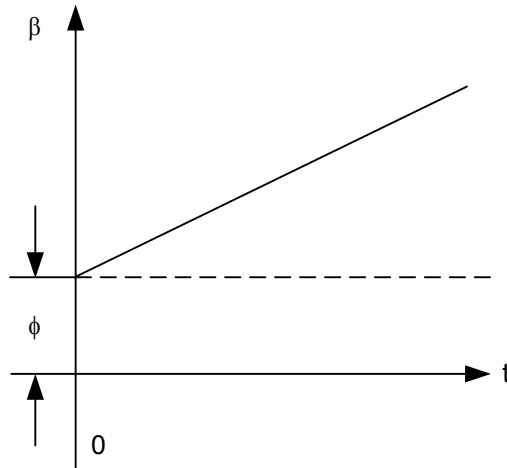


**Figure 3** Phase measurement at off-nominal frequency for  $\Delta f > 0$

If we compare the angle measurement,  $\beta$ , at two locations with constant  $\phi$ , the angle difference,  $\Delta\beta$ , is constant and equal to  $\phi_\Delta$ , as Figure 4 illustrates, provided that the phase angle comparison occurs at exactly the same time.

$$\Delta\beta(t) = \beta_A(t) - \beta_B(t) = \phi_\Delta \quad (10)$$

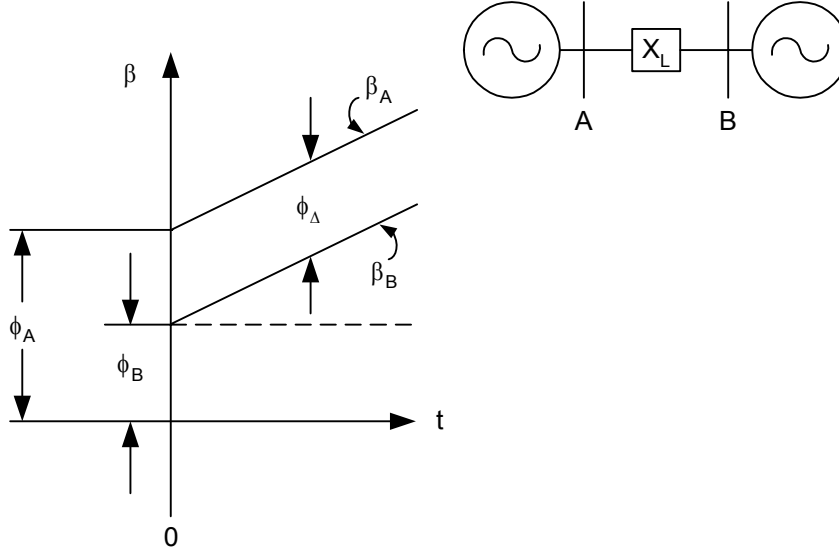


**Figure 4** Phase measurement at two locations at off-nominal frequency

### **Phase as Indicator of the Dynamic Performance of a Power System**

Synchronous machines must adapt to different operating conditions when exchanging real power across a power system [4]. The machines accelerate or decelerate to adapt to changing power transfer requirements that occur during system disturbances. Power system dynamics involve the electrical properties, as well as the mechanical properties, of the electrical machines in the system. For the purpose of this discussion, assume a two-pole synchronous machine where the mechanical and electrical degrees are equal.

The difference between shaft torque,  $T_m$ , and electromechanical torque,  $T_e$ , in a machine determines the accelerating torque,  $T_a$ , as shown by Equation 11. In generators,  $T_a > 0$  accelerates the machine.

$$T_a = T_m - T_e \quad (11)$$

We can represent power,  $P$ , as a function of torque,  $T$ , according to Equation 12.

$$P = T \cdot \omega \quad (12)$$

where:

$T$  is the torque,  $N \cdot m$

$\omega$  is the angular velocity,  $rad/s$

As we see from Equation 13, the change of the angular rotor position,  $\theta$ , with respect to time determines the angular velocity,  $\omega$ .

$$\omega = \frac{d\theta}{dt} \quad (13)$$

The torque,  $T$ , is a function of the moment of inertia,  $J$ , and the angular acceleration,  $\alpha$ , according to Equation 14.

$$T = J \cdot \alpha \quad (14)$$

where:

$J$  is the moment of inertia,  $\text{kg}\cdot\text{m}^2$

$\alpha$  is the change of the angular velocity with respect to time,  $\text{rad/s}^2$

As in Equation 15, the angular momentum,  $M$ , is a function of the moment of inertia,  $J$ , and the angular velocity,  $\omega$ .

$$M = J \cdot \omega \quad (15)$$

With Equation 16, we can represent the accelerating power,  $P_a$ , as a function of the angular acceleration,  $\alpha$ , and as a function of the angular rotor position,  $\theta$ .

$$P_a = T_a \cdot \omega = M \cdot \alpha = M \cdot \frac{d^2\theta}{dt^2} \quad (16)$$

We can express the rotor angle position with respect to a synchronous reference frame that rotates at synchronous speed,  $\omega_{\text{syn}}$ . The angular rotor position,  $\theta$ , is equal to the phase angle due to the synchronous rotating reference,  $\omega_{\text{syn}} \cdot t$ , plus the angular displacement from the synchronous rotating reference,  $\delta$ , as shown in Equation 17.

$$\theta(t) = \omega_{\text{syn}} \cdot t + \delta \quad (17)$$

The angular velocity,  $\omega$ , is:

$$\omega = \frac{d\theta}{dt} = \omega_{\text{syn}} + \frac{d\delta}{dt} \quad (18)$$

Taking the derivative of the angular velocity, we can rewrite Equation 16 as a function of  $\delta$ :

$$P_a = M \cdot \frac{d^2\delta}{dt^2} \quad (19)$$

We can express Equation 19 as a function of the constant inertia,  $H$ , with power expressed in per unit as follows:

$$P_a = P_m - P_e = \frac{2 \cdot H}{\omega_{\text{syn}}} \cdot \frac{d^2\delta}{dt^2} = \frac{2 \cdot H}{\omega_{\text{syn}}} \cdot \frac{d\omega}{dt} \quad (20)$$



where:

$P_m$  is the mechanical power supplied to the generator, pu

$P_e$  is the electrical power supplied to the system, pu

$H$  is the constant of inertia, s

Equation 20 is known as the swing equation; one swing equation per machine is necessary to model the network dynamics. When the load-generation equation is balanced (total load equals total generation), machine speeds are practically equal to synchronous speed.

The angular displacements,  $\delta$ , of machines in a system provide information about the system dynamics. One cannot measure this angular displacement mechanically. By computing the voltage phasor behind the machine transient reactance, one can study the phase angle variations to obtain an image of the machine angular displacement. In practice, machine oscillating modes can be determined by measuring the phase angle of the positive-sequence voltage phasor at the machine terminals. This is demonstrated later in the text.

### **Voltage, Frequency, and Phase Angle**

Frequency carries a special significance when dealing with the measurement of phasors in real time. Phasors are basically a concept applied at a single frequency. In an actual network, situations could develop in which the frequency is other than the rated value.

Equations 18 and 20 determine the speed of a generator, and the generator speed determines the frequency at the generator output. When each generator swing equation reaches equilibrium, the operating frequency is the same on all points of the network, and we can represent a bus voltage, phase angle, and angular velocity with Equations 6, 17, and 18, respectively.

During a network disturbance (fault, loss of generation, or major load change), both the angular velocity and the phase angle undergo local changes. We can rewrite Equation 18 as a function of frequency and phase angle as follows:

$$f = f_{\text{syn}} + \frac{1}{2 \cdot \pi} \cdot \frac{d\delta}{dt} \quad (21)$$

where:

$f_{\text{syn}}$  is the frequency at synchronous speed, Hz

Equation 21 indicates that, during a major disturbance, the local frequency and the local phase angle change simultaneously. We shall see later that this behavior has some direct consequences on the way a phasor measurement is processed in relation to the signal sampling frequency: fixed or adaptive.

### **Phasor Representation in Steady and Transient States**

On a power network, we can define steady state as the situation where generation and load are practically (within an acceptable margin of error) balanced and the load-frequency regulation has reached a point of balance (i.e., network frequency equals rated frequency). In steady state, therefore, voltage and current time waveforms have constant amplitude, frequency, and phase

angle. Although we usually assume the constant frequency in steady state to be the system nominal frequency, that assumption is not always true.

In steady state, measured real-time phasors, according to the original definition, are the solution of any set of network equations under consideration. As an example, consider the positive-sequence voltage (PSV) synchronized phasors at the extremities of a line such as that modeled in Figure 5.

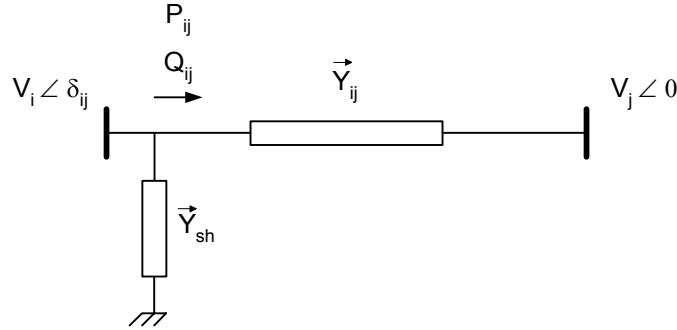


**Figure 5** Line power flow depends on the terminal voltage magnitudes and angles

The relationship between the line real and reactive power flows and the PSV phasors at the line buses is provided by the next two equations:

$$P_{ij} = V_i^2 \cdot \text{real}(\vec{Y}_{sh} + \vec{Y}_{ij}) - V_i \cdot V_j [\text{real}(\vec{Y}_{ij}) \cos \delta_{ij} + \text{imag}(\vec{Y}_{ij}) \sin \delta_{ij}] \quad (22)$$

$$Q_{ij} = -V_i^2 \cdot \text{imag}(\vec{Y}_{sh} + \vec{Y}_{ij}) - V_i \cdot V_j [\text{real}(\vec{Y}_{ij}) \sin \delta_{ij} - \text{imag}(\vec{Y}_{ij}) \cos \delta_{ij}] \quad (23)$$

Computation of synchronized phasors in real time occurs through the use of filtering systems [5, 6, 7, 8]. In steady state, a phasor value is independent from the filtering system; different filtering systems provide the same output.

We can define transient state on a power network as the condition in which the magnitude, phase angle, or frequency of one or more bus voltages become a function of time. Another definition of transient state could be the network condition existing between two stable states. This means that every time a change occurs on a network, a transient state condition will follow. Phasors, by definition, cannot represent in transient state the exact value of corresponding variables. The amount of transient error will to a great extent depend upon filtering system frequency tracking capability, which in turn depends upon response time and frequency response.

In transient state, one has to expect that two different filtering systems will provide different outputs. Although synchronized phasors will exhibit some errors in transient state, the level of errors is usually acceptable; transient state applications should be considered viable and reliable. The situation is similar to that of applying phasors in protective relaying: voltage and current phasors, although computed in transient state, still perform the task of detecting faults.

## PRESENT SAMPLING AND SIGNAL PROCESSING PRACTICES

Following is a brief description of present sampling and signal processing practices for synchronized phasor measurement, oscillography, harmonic analysis, and line distance protection. First, we describe sampling at fixed time intervals (constant number of samples per

second) without and with an absolute time reference. Then, we discuss sampling at multiples of power system operating frequency (constant number of samples per power system cycle).

### Sampling at Fixed Time Intervals

Traditionally, digital fault recorders (DFRs) acquire data at fixed time intervals to provide voltage and current oscillography and harmonic analysis. For example, DFRs use sampling rates ( $f_s$ ) of 1 kilosample/second (kSPS) or faster. The samples are synchronized to an internal time source or an external time source. In some applications, the external time source is an absolute time reference from a global positioning system (GPS) receiver. Figure 6 shows a typical DFR data acquisition block diagram with traditional DFR applications (such as oscillography and harmonic analysis) using an internal time source. The figure includes a hardware low-pass filter (Hardware LPF) for anti-aliasing and an analog-to-digital (A/D) converter for analog-to-digital conversion.

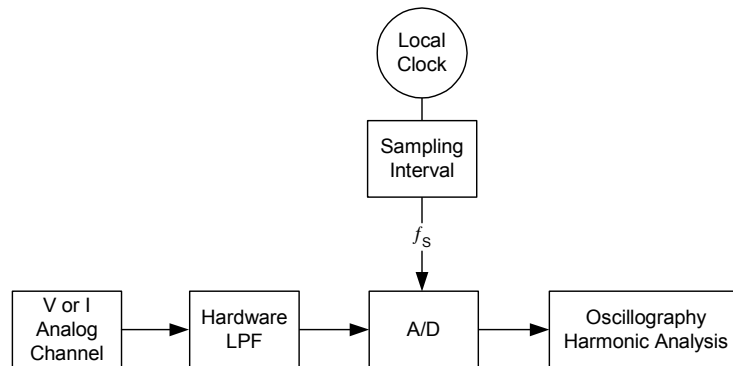


**Figure 6** Sampling at fixed time intervals with a local clock for oscillography and harmonic analysis

The main advantage of this acquisition system is that the data preserve the frequency information of the power system. For example, you can analyze power system frequency excursions during power system disturbances. This data acquisition system is also suitable for synchronized phasor measurement (Figure 7) when an external time source with absolute time reference determines the sampling interval [9].

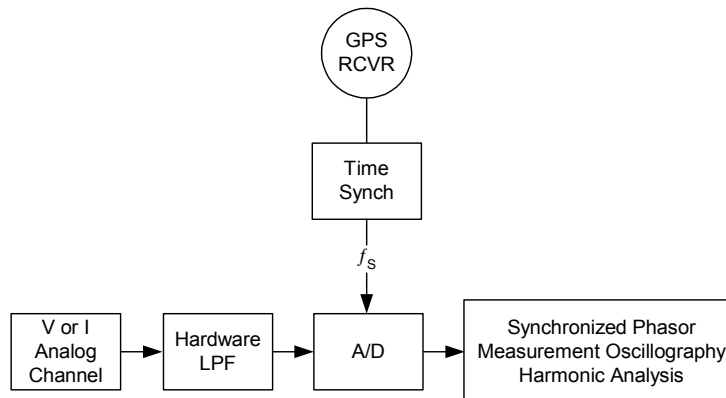


**Figure 7** Sampling at fixed time intervals with an absolute time reference for synchronized phasor measurement, oscillography, and harmonic analysis

A small variation of this approach is a sampling system that uses a fixed sampling rate ( $f_s$ ) that is a multiple of the system nominal frequency ( $f_{\text{NOM}}$ ). For example, 960 samples/second (SPS) could be the sampling rate. This rate is 16 times the nominal frequency ( $f_{\text{NOM}}$ ) in a 60 Hz power system.

Sampling at constant time intervals is suitable for multiple protection applications such as current differential protection [10], but it introduces unwanted errors in protection applications such as line distance protection. One common approach to obtaining phasor information for protection applications is to calculate the Discrete Fourier Transform (DFT) of the sampled signal. It is well documented in the literature [11] that this phasor calculation is in error when the power system operates at off-nominal frequencies. Figure 8 shows the deviation from ideal of the phasor calculation for angles from  $0^\circ$  to  $360^\circ$ . These calculation errors may cause distance element misoperation [12]. The data acquisition system requires information about the power system operating frequency to minimize phasor calculation errors, as we will see later.

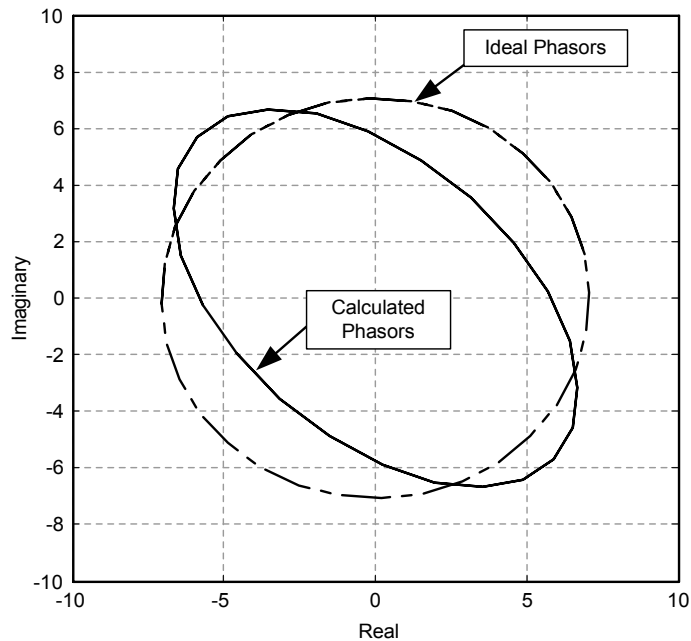


**Figure 8** Phasor calculation errors at off-nominal frequency

### **Sampling at Multiples of Power System Operating Frequency**

Sampling at multiples of power system operating frequency minimizes phasor calculation errors when the system operates at off-nominal frequencies. Figure 9 shows this type of data acquisition system. The system calculates the power system operating frequency ( $f_{\text{SYS}}$ ) and uses this frequency information to obtain the sampling frequency ( $f_s$ ) as a multiple of the system operating frequency. Reference [13] describes one method of frequency estimation; other frequency estimation approaches accomplish the same task [11]. The sampled data pass through a digital band-pass filter (DBPF), after which the filtered signal is ready for line distance protection applications. This approach reduces errors in phasor calculations; remaining error depends only on frequency estimation error, usually less than 0.01 Hz. A disadvantage of this approach is that the phasor measurement is not referenced to absolute time for synchronized phasor measurement applications. The approach needs an absolute time reference for such applications.

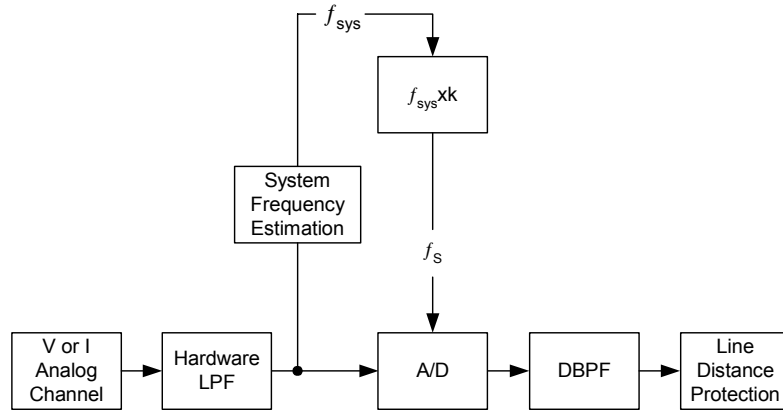


**Figure 9** Sampling at multiples of power system operating frequency for line distance protection

### Sampling at Fixed Time Intervals With Adaptive Filtering

We can use samples at fixed time intervals to calculate phasors with minimum error. In this approach (see Figure 10), the data acquisition system estimates the power system operating frequency and uses this frequency information to modify the filter coefficients of the digital band-pass filter. This approach is attractive because it minimizes errors in phasor calculations without needing a constant number of samples per cycle. A disadvantage of this approach is that it does not provide a common time reference for multiple devices connected at different power system locations. The approach is also not suitable for synchronized phasor measurements. US Patent Number 6,141,196 [14] describes one method that uses a similar approach.

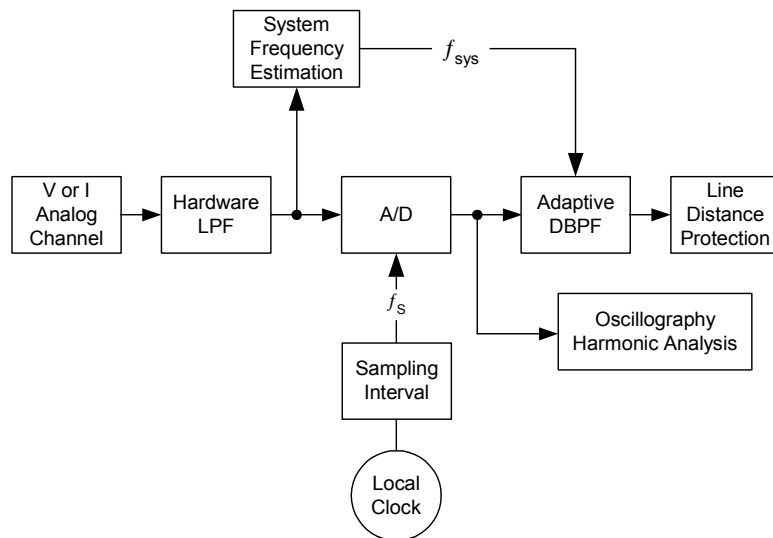


**Figure 10** Sampling at fixed time intervals with adaptive filtering for oscillography, harmonic analysis, and line distance protection

## **SAMPLING AND SIGNAL PROCESSING FOR SYNCHRONIZED PHASOR MEASUREMENT AND LINE DISTANCE PROTECTION (PATENT PENDING)**

The data acquisition methods we discussed earlier provide solutions suitable for either synchronized phasor measurement applications, which require sampling referenced to an absolute time reference, or line distance protection applications, which require sampling at multiples of the power system operating frequency. Figure 11 shows data acquisition and data processing suitable for both kinds of applications. This data acquisition and processing system is part of a multiple power system applications device that we describe in the following sections.

### **Sampling and Signal Processing for Multiple Power System Applications**

The multiple applications device acquires data at fixed time intervals; the sampling frequency ( $f_s$ ) depends on an external clock signal (GPS receiver) with absolute time reference. For synchronized phasor measurement applications, the device uses the GPS time reference. After the A/D converter acquires the data, the data are calibrated to compensate for hardware data acquisition errors. The calibrated data ① are available at a high sampling rate (e.g. 8 kSPS); these data are suitable for synchronized phasor measurements, oscillography, and harmonic analysis applications. The high sampling rate data pass through a digital low-pass filter (DLPF) ② before down sampling and resampling. The down sampler outputs data at a lower rate ③ for frequency estimation. One of the inputs to the resampler (RSMP) is the filtered signal ②. The second input to the resampler is the power system operating frequency ( $f_{SYS}$ ) ④. The resampler outputs data ⑤ at a rate that is a multiple of the operating frequency ( $f_{SYS}$ ), e.g.,  $32 \cdot f_{SYS}$ . The resampled data pass through a digital band-pass filter (DBPF). The DBPF has fixed coefficients that do not depend on the power system operating frequency ( $f_{SYS}$ ). The filtered data ⑥ are ready for distance protection applications such as Reference [15] describes. The filtered data are also available to calculate the magnitude of the synchronized phasor, as we will see later.

Figure 12 shows a variation of this sampling and signal-processing system, in which the sampling is based on the local clock. Resampling in this variation uses the absolute time reference from the GPS receiver and the system operating frequency to resample the data at a specific frequency depending on application requirements.

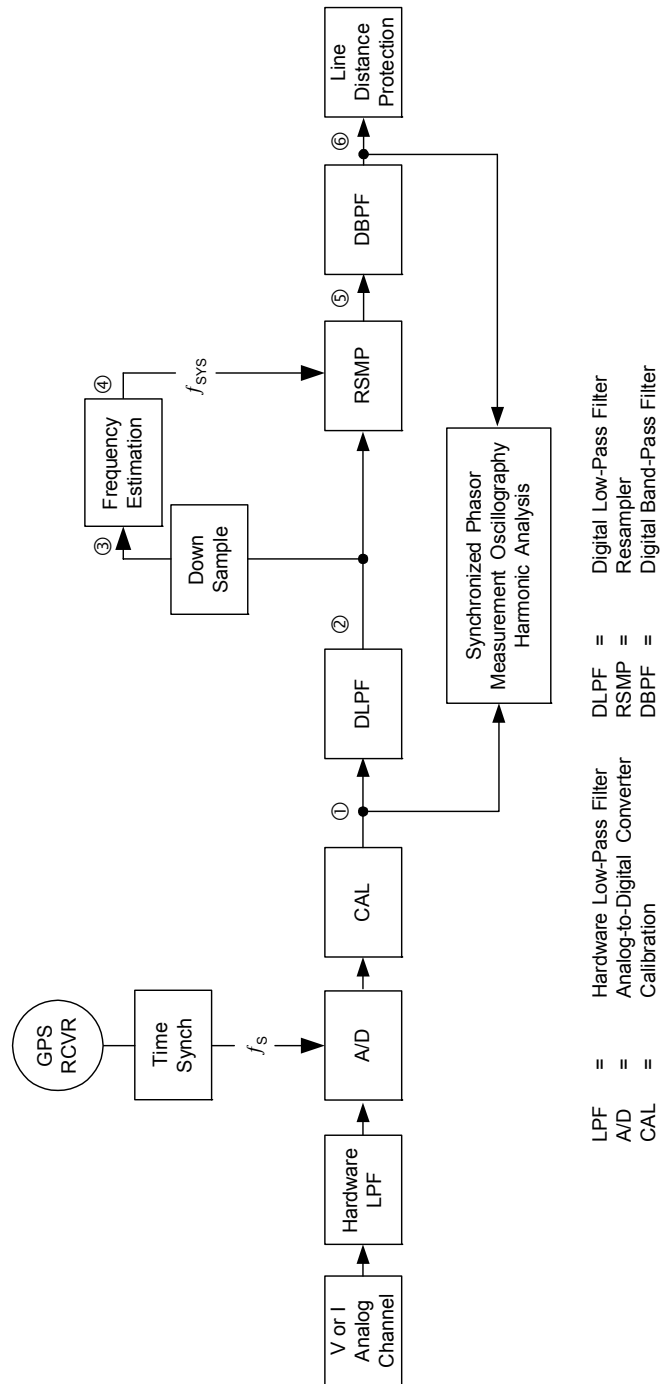


**Figure 11** Sampling with an absolute time reference for synchronized phasor measurement applications and resampling at multiples of the power system operating frequency for line distance protection applications

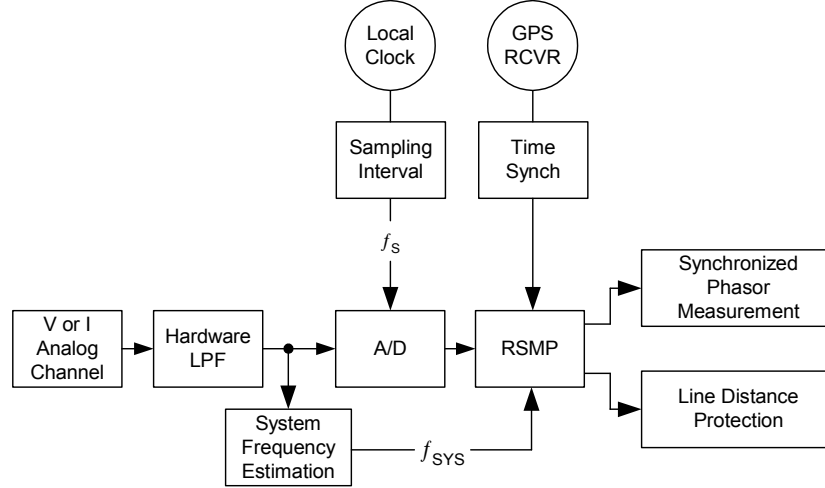


**Figure 12** Sampling at fixed time intervals with a local clock, and resampling according to the absolute time reference and power system operating frequency

### **An Algorithm Decoupling Phasor Magnitude and Phase Angle Measurements**

Considering that a system with adaptive sampling allows measurement of a phasor magnitude over a broad frequency interval and that a system with a fixed sampling frequency allows avoidance of the local frequency measurement, combination of these two systems would optimize phasor measurement performance. Such a system is shown in Figure 13. Consider the voltage waveform of Equation 6 and assume multiplication of this waveform by a time-synchronized unit phasor, according to the following equation:

$$\vec{V} = V \cdot \cos(2 \cdot \pi \cdot f_{\text{NOM}} \cdot t + \phi) e^{-j2\pi f_{\text{NOM}} t} \quad (24)$$

which can be otherwise expressed as Equation 25:

$$\vec{V} = \frac{V}{2} [e^{j2\pi f_{\text{NOM}} t} \cdot e^{j\phi} + e^{-j2\pi f_{\text{NOM}} t} \cdot e^{-j\phi}] e^{-j2\pi f_{\text{NOM}} t} \quad (25)$$

or as Equation 26:

$$\vec{V} = \frac{V}{2} [e^{j\phi} + e^{-j4\pi f_{\text{NOM}} t} \cdot e^{-j\phi}] \quad (26)$$

If we filter out the double-frequency component, we finally obtain Equation 27:

$$\vec{V} = \frac{V}{2} \cdot e^{j\phi} \quad (27)$$

The computed phasor is the original waveform phasor with the magnitude divided in half. Because we use a signal at synchronous speed to demodulate the input signal, the magnitude of the computed phasor will not represent properly the magnitude of the incoming signal at off-nominal frequency. To obtain a phasor magnitude evaluation independent of frequency, we use the magnitude of the phasor calculation for protective functions that has been processed through a system with adaptive sampling frequency. The final phasor combines the two outputs: magnitude on one side and phase angle on the other. The unit exponential function that multiplies the signal has a fixed sampling frequency of 1 kHz and is time synchronized.



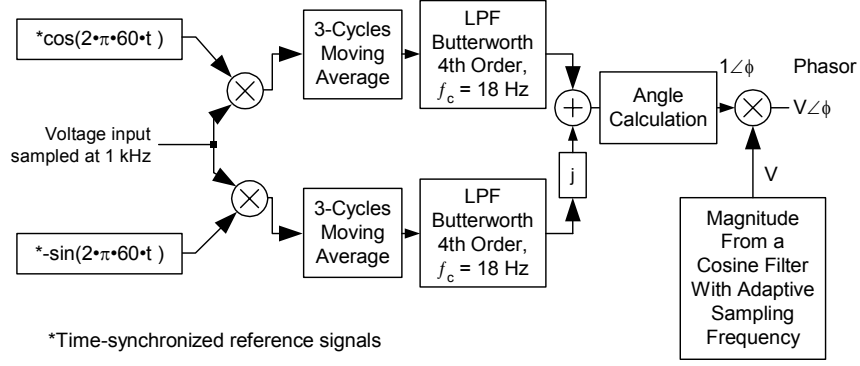


**Figure 13** Principle of decoupled-phasor measurement

### Performance of the Decoupled Algorithm

We first evaluate the capability of the decoupled algorithm to perform phase angle measurement outside rated frequency. Equation 28 and Equation 29 define two waveforms  $v_1(t)$  and  $v_2(t)$ :

$$v_1(t) = \cos(2 \cdot \pi \cdot 59.5 \cdot t + \pi/4) \quad (28)$$

$$v_2(t) = \cos(2 \cdot \pi \cdot 59.5 \cdot t) \quad (29)$$

These waveforms are processed through the decoupled algorithm, and the resulting phase angles are shown in Figure 14.

One can see that, in both cases, the rate of change of the phase angles is constant and equal to  $-180^\circ/s$ :

$$\frac{d\phi_1}{dt} = \frac{d\phi_2}{dt} = -\pi \text{ rad/s} = -180^\circ/\text{s} \quad (30)$$

After the transient response has faded away, Equation 31 provides the steady-state phase angle difference between the two phasors at any synchronous time:

$$\phi_1 - \phi_2 = \frac{\pi}{4} \text{ rad} = 45^\circ \quad (31)$$

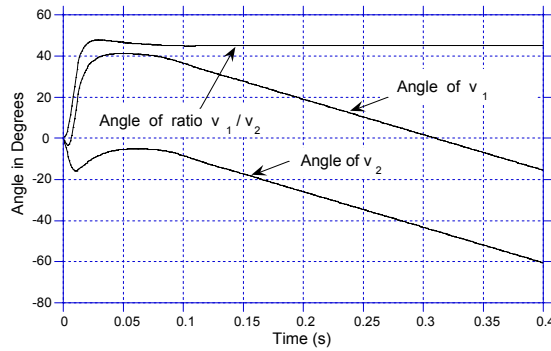


**Figure 14** Phase angle difference between two phasors at off-nominal frequency

To evaluate the dynamic performance of the decoupled algorithm, we will revisit the classic problem of a generator connected to an infinite bus through a transmission line for different operating and fault conditions. Figure 15 shows the network, which has been modeled with the Power System Blockset [1]. Both the power-frequency and the field supply-regulation loops have been modeled as shown in Figure 16. The speed-droop characteristic (percent change in frequency that would cause the output power of the unit to change by 100 percent) has been set to 5 percent.

Three-phase faults of different durations applied at the output of a generator induce frequency oscillations on the machine. Frequency oscillations resulting from a difference between the mechanical and electrical power (Equation 20) are known to be stable (the frequency returns to a stable and constant value) or unstable (the frequency steadily increases or decreases). We could use the equal-area algorithm [4] to analyze this example theoretically. We will demonstrate, instead, that by measuring the difference in phase angle between the PSV phasor at the output of the generator (Bus 1) and the same phasor at the infinite bus (Bus 3), it is possible to detect transient stability or instability conditions. Note that although this application of synchronized phasors is in transient state (the frequency close to the generator is a function of time), it nevertheless achieves the primary goal of measuring the phase angle between two bus voltages.

A three-phase short circuit is applied at Bus 2 for 50 ms, with the resulting machine speed shown in Figure 17. Ultimately, the machine speed returns to its synchronous value. The frequency disturbance is reflected in the voltage phase angle close to the machine. Figure 18 shows the phase angle difference between the two synchronized PSV phasors measured at Bus 1 and 3 using the phasor-decoupling algorithm. Obviously, the phase angle disturbance is also stable.

Figure 19 and Figure 20 show the results of the same simulation with a three-phase fault applied for 200 ms. The speed and PSV phasor phase angle difference time waveforms reflect a stable disturbance for a second time, although the excursion amplitudes are much larger than the previous example.

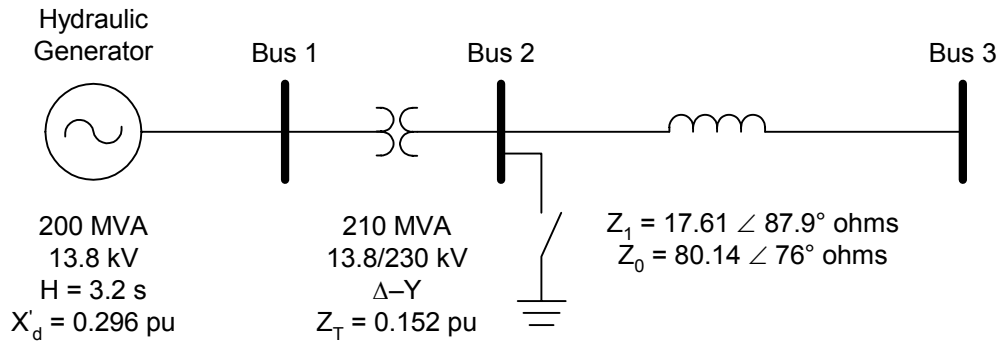


**Figure 15** Generator and infinite-bus network model

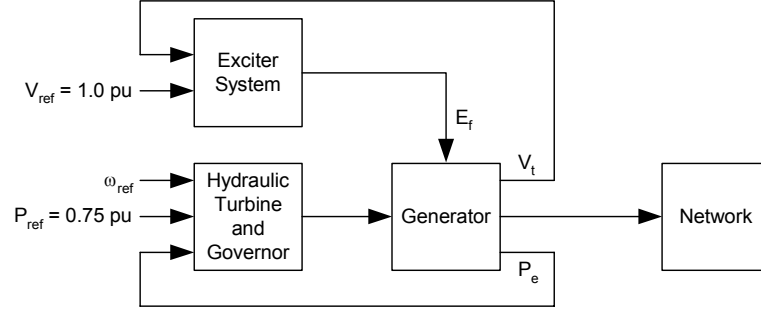


**Figure 16** Generator voltage and hydraulic-turbine regulators model

Figure 21 and Figure 22 show the machine speed and the phase angle difference between the PSV phasors measured at Bus 1 and Bus 3, respectively, for a 300 ms fault. This fault duration is longer than the critical clearing time. In this case, the system becomes unstable; the phase difference corresponds to an increasing exponential with a positive time constant. The plot of the machine speed shows a linearly increasing angular velocity, which indicates loss of machine synchronism with respect to the infinite bus frequency.

The generator rotor swing equation for this particular system is provided by Equation 20, which can be otherwise expressed as Equation 32:

$$\frac{2H}{\omega_{\text{syn}}} \frac{d^2\delta}{dt^2} = P_m - P_{\text{max}} \cdot \sin \delta \quad (32)$$

where the following provides maximum power  $P_{\text{max}}$ :

$$P_{\text{max}} = \frac{E'_1 \cdot E_3}{X_{13}} \quad (33)$$

where:

$E'_1$  is the generator voltage magnitude behind the transient reactance  $X'_d$

$E_3$  is the infinite bus voltage source magnitude

$X_{13}$  is the reactive impedance magnitude between the two voltage sources

We can use Equation 34 to calculate the reactive impedance between the two sources:

$$X_{13} = X'_d + X_T + X_L + X_S \quad (34)$$

where:

$X'_d$  is the generator transient reactance

$X_T$  is the transformer reactance

$X_L$  is the line reactance

$X_S$  is the infinite bus source reactance

with the following circuit values:

$$X_{13} = 0.296 + 0.152 + 0.066 + 0.02 = 0.536 \text{ pu} \quad (35)$$

Given that the mechanical power supplied to the generator is 0.75 pu, and with the magnitude of the two sources equal to unity, we can use Equation 36 to compute the swing equation at the point of balance:

$$\frac{2H}{\omega_{\text{syn}}} \frac{d^2\delta}{dt^2} = 0.75 - 1.866 \cdot \sin 23.70^\circ \quad (36)$$

During a disturbance, the oscillation frequency of the generator rotor is provided by [4]:

$$f_n = \frac{1}{2\pi} \sqrt{\frac{\omega_s \cdot S_p}{2 \cdot H}} = \frac{1}{2\pi} \sqrt{\frac{377 \cdot 1.707}{2 \cdot 3.2}} = 1.597 \text{ Hz} \quad (37)$$

where  $S_p$  is the synchronizing power coefficient calculated by Equation 38:

$$S_p = \left. \frac{dP_e}{dt} \right|_{\delta=\delta_0} = P_{\text{max}} \cdot \cos \delta_0 = 1.866 \cdot \cos 23.70^\circ = 1.707 \text{ pu} \quad (38)$$

The theoretical period,  $1/f_n$ , of oscillation is 0.626 seconds. The measured period of oscillation for the 50 ms fault is 0.633 seconds, while the period for the 200 ms fault is 0.643 seconds. In both cases, the error is less than 3 percent.

This example demonstrates the following:

1. Although the example can be considered a transient-state condition, the synchronized phasor measurement provides fairly good accuracy for measurement of the phase angles.
2. The accuracy achieved in computing the phase angle of the phasors shows that the fixed sampling frequency (1 kHz) is particularly efficient for resolving the phase angle difference between signals that are not at rated frequency.

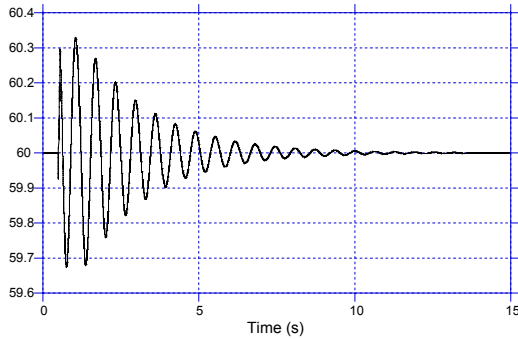


**Figure 17** Machine speed or frequency for a 50 ms fault

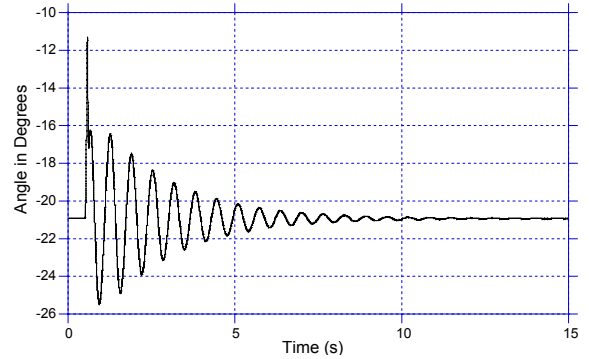


**Figure 18** PSV phasors phase angle difference between buses for a 50 ms fault

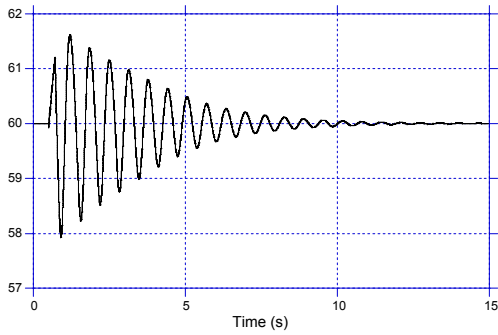


**Figure 19** Machine speed or frequency for a 200 ms fault

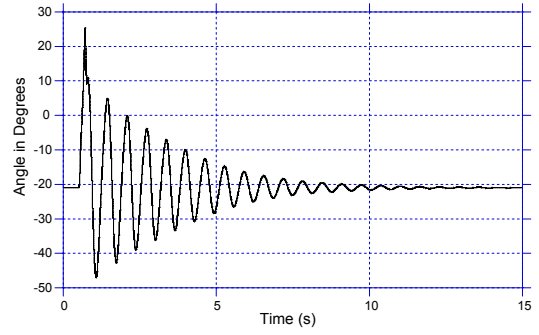


**Figure 20** PSV phasors phase angle difference between buses for a 200 ms fault

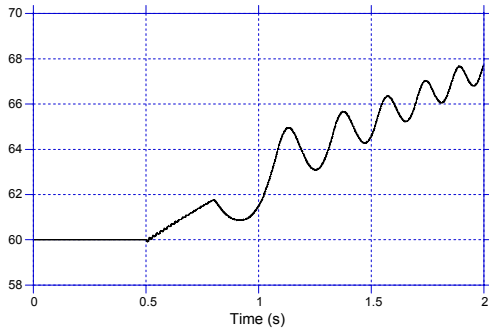


**Figure 21** Machine speed or frequency for a 300 ms fault

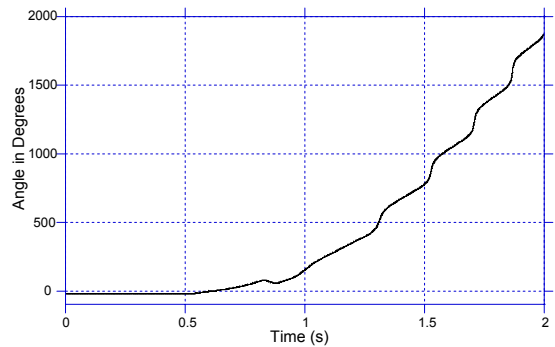


**Figure 22** PSV phasors phase angle difference between buses for a 300 ms fault

## SYNCHRONIZED PHASOR APPLICATIONS

### Real-Time Monitoring of State Variables

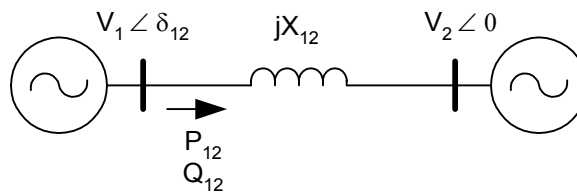


**Figure 23** Elementary single-line network

Real-time implementation of synchronized phasors allows for the fast measurement of PSV phasors at network buses. The phase angles of these quantities constitute the most important network state variables, because these angles are related to the network transient stability margin, line power flows, and voltage security [16, 17].

For the elementary line represented in Figure 23, the equation for the real power flow at the left bus is given by the conventional real power flow equation:

$$P_{12} = \frac{V_1 \cdot V_2}{X_{12}} \sin \delta_{12} \quad (39)$$

and by the conventional reactive power flow equation:

$$Q_{12} = \frac{V_1^2}{X_{12}} - \frac{V_1 V_2}{X_{12}} \cos \delta_{12} \quad (40)$$

Equations 39 and 40 are identical to Equations 22 and 23, except that the shunt admittance and line resistance are considered negligible. To establish the relationship among the voltage regulation (expressed as the ratio of the two voltage magnitudes at the line extremities), the reactive power supplied to the line, and the phase angle between the voltage phasors, Equation 40 takes the form of Equation 41:

$$\frac{V_2}{V_1} = \frac{V_1^2 - X_{12} \cdot Q_{12}}{V_1^2 \cdot \cos \delta_{12}} \quad (41)$$

We can express the remote voltage,  $V_2$ , in per unit for  $\bar{V}_1 = 1 \angle 0^\circ$  as follows:

$$V_2 = \frac{1 - X_{12} \cdot Q_{12}}{\cos \delta_{12}} \quad (42)$$

Monitoring of network state variables allows also for verification and calibration of network studies.

### **Phase Transducer and Dynamic Recording of Phases**

Any change occurring on an electrical network (i.e., network fault), topological change such as the opening or closing of a line, step changes in generation-load equilibrium (loss of a generation block or addition of a major load), tie-line or inter-area stable or unstable power oscillations, etc., will be reflected in the measurement of the magnitude and the phase angle of the network state variables.

Recording of strategically located phase angle state variables prior and after the disturbance provides valuable information about the power system response and the capacity of the power system to respond to adverse events.

### **Special Protection Systems and Network Out-Of-Step Relaying**

A number of utilities have ongoing projects or have already used synchronized phasor principles to monitor network transient stability or to implement special protection systems based on out-of-step protection.

When a number of network generators start to run at different speeds, loss of synchronism might occur. When one portion of a network becomes unsynchronized with respect to another, the voltage phase at the buses close to the generators causing the disturbance reflects changes in rotation speed. When a protection system detects instability, remedial action schemes can involve network separation or load shedding.

Two approaches have been described to implement a network out-of-step application [18, 19, 20, 21]:

1. To the extent that a two-machine system equivalent can represent a network, one approach consists of synchronous measurement of the phase angle between the transient reactances of the two machines. When a disturbance occurs, the new phase angle between the two machines is computed and the equal area algorithm is implemented in real time to determine whether the new point of operation is stable [19, 20].
2. A second approach consists of measuring the PSV phasors at two or more strategically located buses. During a disturbance, the phase angle between the signal pairs is computed in real time, and a predictive algorithm is used to establish whether the disturbance will be stable. One application uses a model of the phase angle time waveform in the form of an exponentially damped sine wave [21]:

$$\delta(t) = \delta_0 + A \cdot e^{-\alpha t} \cdot \sin(\omega t + \beta) \quad (43)$$

where  $\delta_0$  is the initial phase difference,  $\alpha$  is a damping constant,  $\omega$  is the angular frequency of the phase difference, and  $A$  is the oscillation amplitude. A predictive algorithm is used to identify the phase angle variation parameters and to determine stability or instability conditions.

### **State Estimation**

The purpose of a state estimation program [22, 23] in a Network Management Center is to provide a statistical real-time estimate of network state variables in the form of bus voltage magnitudes and phase angles. A state estimator can detect and correct gross measurement errors. State estimation is a steady-state application and a slow process, with a time frame on the order of a few minutes.

A number of synchronous measurements are taken in real time on the network. The state variables are computed from the set of nonlinear equations linking the measurements to the state variables. The process is statistical because there are normally more measurements than state variables, and an increased number of measurements improves the accuracy of the result.

As an example, consider the network of Figure 23. It is clear that actual networks and the extent of computations will be much larger than the example shows.

First, a state variable vector is defined as the PSV phasor magnitude of the two buses and the phase angle between these buses [23]:

$$x = \begin{bmatrix} x_1 \\ x_2 \\ x_3 \end{bmatrix} = \begin{bmatrix} \delta_{12} \\ V_1 \\ V_2 \end{bmatrix} \quad (44)$$

Then, vector  $z$  of the measurements is defined. The measurements include the magnitude of the two PSV phasors and the line power flows,  $P_{12}$  and  $Q_{12}$ . Assuming that synchronous phasors are available on this network, the phase angle between the bus voltages,  $\delta_{12}$ , is now available, and the measurement vector is as shown in Equation 45:

$$z = \begin{bmatrix} \delta_{12} \\ V_1 \\ V_2 \\ P_{12} \\ Q_{12} \end{bmatrix} + \begin{bmatrix} \varepsilon_1 \\ \varepsilon_2 \\ \varepsilon_3 \\ \varepsilon_4 \\ \varepsilon_5 \end{bmatrix} \quad (45)$$

The  $\varepsilon$  vector represents an assumed error between the measurement and the true value. The relationship between the measurement and the state variables is provided by a set of non-linear equations  $h(x)$  as in Equation 46 (after application of Equations 39 and 40):

$$z = h(x) + \varepsilon = \begin{bmatrix} x_1 \\ x_2 \\ x_3 \\ \frac{x_2 \cdot x_3 \cdot \sin x_1}{X_{12}} \\ \frac{x_2^2 - x_2 \cdot x_3 \cdot \cos x_1}{X_{12}} \end{bmatrix} + \begin{bmatrix} \varepsilon_1 \\ \varepsilon_2 \\ \varepsilon_3 \\ \varepsilon_4 \\ \varepsilon_5 \end{bmatrix} \quad (46)$$

It is beyond the scope of this paper to discuss the solution (minimize  $\varepsilon$ ) for this type of nonlinear set of equations. Let us just mention that one possible solution is the Weighted Least Squares technique, which, after assuming an initial state variable vector, uses the following recursive formula to repetitively compute the final result [24]:

$$x^{k+1} = x^k + [H(x^k)^T \cdot R^{-1} \cdot H(x^k)]^{-1} H(x^k) \cdot R^{-1} [z - h(x^k)] \quad (47)$$

In this equation,  $R$  is the measurement diagonal covariance matrix, and  $H(x^k)$  is the measurement Jacobian matrix. Following initialization of the state variable vector, the computation uses the measured values of the phase angles as starting values.

## SYSTEM CONSIDERATIONS

Synchronously sampled event records simplify system-wide disturbance analysis. These records include system dynamic information that can be used to evaluate system conditions and compare these conditions to system models. Synchronized phasor measurement reports that include phasor information at specific instants of time allow a host computer to parse the measurements from different system locations for system-wide control and protection applications automatically.

### Synchronously Sampled Data Recording for System-Wide Disturbance Analysis

To provide synchronously sampled event records, the multiple applications device generates a time stamp for each acquired sample. The device requires two signals from the GPS receiver: the one kilo-pulse per second (1kPPS) signal and the IRIG-B signal [25]. The 1kPPS signal is a periodic pulse train at a rate of one pulse per millisecond (1 kHz), and the IRIG-B signal is a periodic pulse train at a rate of one time mark per second that includes the start of the second time value. The 1kPPS signal determines when to acquire the sample of the voltage or current signal, and the IRIG-B signal provides the time stamp for the acquired sample. The device uses the sampling clock signal (a signal with a frequency that is a multiple of the 1kPPS signal frequency) and the IRIG-B signal to generate the sample time stamp (see Figure 24). The samples and



corresponding time stamps are available from the communications ports in COMTRADE format [26]. With these multiple applications devices, we can acquire event reports at different power system locations with simultaneously acquired samples, as Figure 25 shows. We can use these synchronously sampled event records to analyze system-wide disturbances faster than if we tried to synchronize the event records manually.

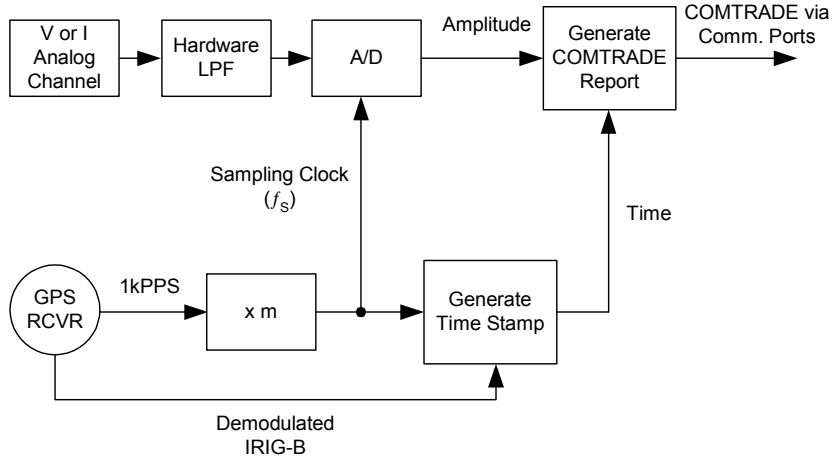


**Figure 24** Synchronously sampled event recording time stamping and report generation

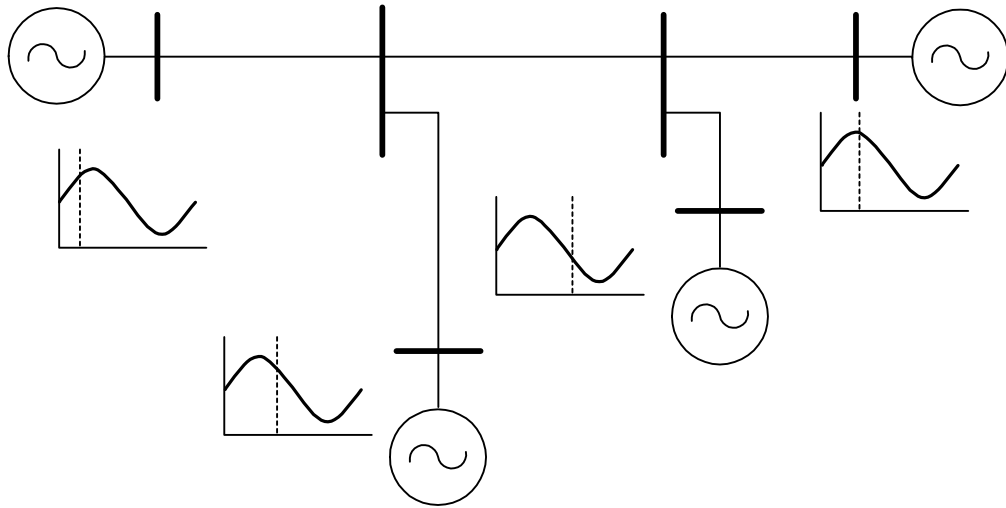


**Figure 25** Synchronous sampling at different power system locations simplifies power system disturbance analysis

### **Data Reporting for Synchronized Phasor Measurement Applications**

The multiple applications device reports the synchronized phasor measurement data in two ways: unsolicited binary messages at specific time intervals and solicited ASCII reports at specific instants of time.

## Unsolicited Binary Messages

Figure 26 shows two relays with synchronized phasor measurement capabilities at different power system locations connected to a remote host computer through communications channels. The host computer enables, disables, and accepts unsolicited binary messages from the relays. The host computer determines the data transfer rate, which depends on the communications bandwidth and the amount of data the relays transmit. The unsolicited binary message contains the following data [27]:

1. Address of the synchronized phasor measurement data. The host computer uses this address to determine the data source.
2. Sample number according to [2].
3. Data acquisition time stamp in Second-of-Century [2].
4. Power system estimated frequency.
5. Phase and positive-sequence voltages (IEEE 32-bit floating point number).
6. Phase and positive-sequence currents (IEEE 32-bit floating point number).
7. Indication that time-synchronization is OK.
8. Indication that the data packet is OK.
9. Fourteen general purpose bits.
10. CRC-16 error detection code to validate the message.

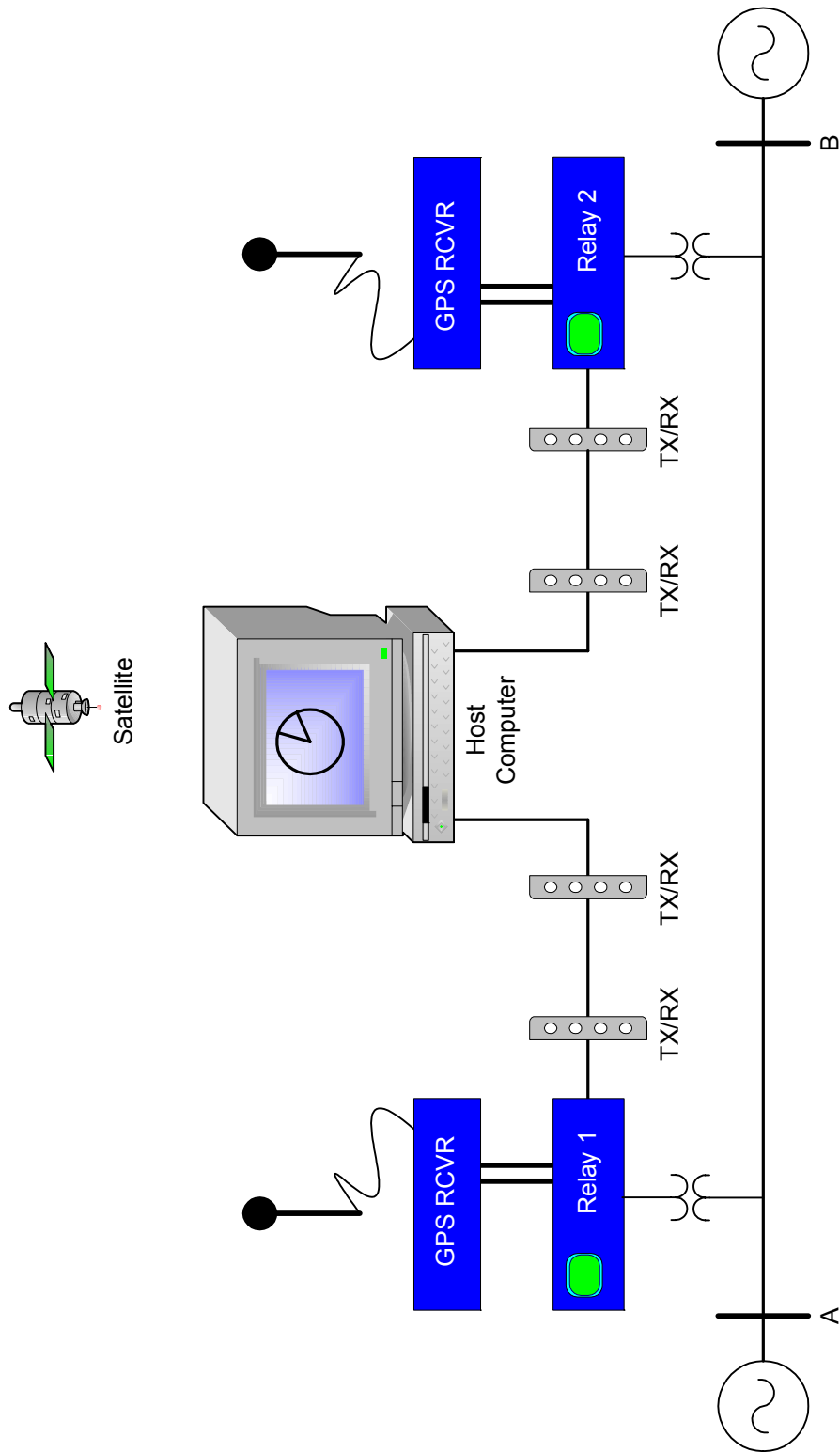


**Figure 26** Relay and host computer connections for synchronized phasor measurement applications

The host computer parses the received data from the different network relays according to the time stamp and sample number of the data packet.

### Solicited ASCII Messages

The relays respond to the **METER PM TIME** command by reporting synchronized phasor measurement at specific times. We can use this command to take snapshots of the phasor at specific times across the power system. Figure 27 shows a sample report.

```

=>>MET PM 6:05
Synchronized Phasor Measurement Data Will be Displayed at 6:05:00.000
=>>

Relay 1                               Date: 01/01/2002 Time: 06:05:00.000
Station A                             Serial Number: 0000000000

Synchronphasors      Phase Currents          Phase Voltages
                    IA      IB      IC      VA      VB      VC
MAG (A/kV)           199.429  201.079  201.392  132.775  132.800  132.784
ANG (DEG)            -134.82  104.69  -14.94   150.00   30.01   -89.99

                    Pos. Sequence Current (A)      Pos. Sequence Voltage (kV)
                    I1                               V1
MAG                  200.632                               132.786
ANG (DEG)            -135.01                               150.00

FREQ (Hz)            59.99

PSV57  PSV58  PSV59  PSV60  PSV61  PSV62  PSV63  PSV64
  0      0      0      0      0      0      0      0
=>>

```

**Figure 27** Solicited ASCII synchronized phasor measurement report

## SOURCES OF ERRORS IN PHASOR ESTIMATION

Synchronized phasor measurement applications such as state estimation and out-of-step relaying require phasor estimation errors on the order of tenths of a degree [9]. Typical sources of these errors include GPS transmitters and receivers, instrument transformers, and phasor estimation devices. We can divide errors from these sources into two categories: time synchronization errors and data acquisition errors. GPS transmitters, GPS receivers, and phasor estimation devices determine time synchronization errors; instrument transformers and phasor estimation devices determine data acquisition errors. Table 1 summarizes these errors and includes typical corresponding values that we must consider in these applications.

**Table 1 Errors in Synchronized Phasor Estimation and Typical Corresponding Values**

Error Cause	Error in Degrees	Error in $\mu$ s
Time Synchronization	$\pm 0.0216$	$\pm 1$
Instrument Transformers (Class 0.3) [28]	$\pm 0.3$	$\pm 14$
Phasor Estimation Device	$\pm 0.1$	$\pm 5$

We can see from Table 1 that instrument transformers are the main contributors to synchronized phasor estimation error. In the near future, we will see technological advances that will minimize these errors.

## CONCLUSIONS

1. Phasors were introduced to transform differential equations, modeling electrical circuits, into common algebraic equations and speed up the solution in steady state.
2. Digital fault recorders acquire data at fixed time intervals. These data retain power system frequency information during off-nominal frequency system operations that can occur during system disturbances.
3. Synchronized phasor measurement devices require an absolute time reference for power system-wide applications. Traditionally, this capability is part of a dedicated device for these applications. These devices are not suitable for protection applications such as line distance protection.
4. The 1kPPS signal provides an absolute time reference for fixed frequency sampling. In synchronized phasor measurement applications, all network waveforms are compared to a time-based phase reference.
5. Phasor calculations using DFT introduce errors when the power system operates at off-nominal frequency. These calculation errors may cause distance element misoperations.
6. Traditionally, numerical relays for line distance protection applications sample voltage and current signals at multiples of the operating power system frequency ( $f_{SYS}$ ) to minimize phasor calculation errors.
7. Data-acquisition systems that acquire data at fixed time intervals and use adaptive filtering minimize phasor calculation errors, but these systems do not sample with a system-wide time reference.
8. A method to acquire and process voltage and current signals for applications such as fault recording, synchronized phasor measurement, and line distance protection samples the signals at fixed time intervals with respect to an absolute time reference and resamples these signals at multiples of power system operating frequency. A simple digital band-pass filter with fixed coefficients provides filtering for the resampled data. Synchronized phasor measurement uses the sampled data with the absolute time reference. Distance protection uses filtered resampled data that minimize phasor calculation errors.
9. In a variation of the approach in Conclusion 8, sampling is based on the local clock. Resampling uses the absolute time reference from the GPS receiver and the system operating frequency to resample the data at a specific frequency depending on the application requirements.
10. Decoupling the magnitude and phase angle measurement provides for an accurate phasor magnitude over a broad frequency interval.
11. Careful calculation of real-time phasors achieves viable accuracy, even in transient states.
12. The multiple-applications device uses unsolicited binary messages and solicited ASCII messages to report synchronized phasor measurement data.

## REFERENCES

- [1] Power System Blockset, The MathWorks, Inc., September 2000, Release 12.
- [2] IEEE Standard 1344-1995. "IEEE Standard for Synchrophasors for Power Systems."
- [3] R. E. Wilson, "Methods and Uses of Precise Time in Power Systems," IEEE/PES Summer Meeting 1991, San Diego, CA.
- [4] W. D. Stevenson, Jr., Elements of Power System Analysis, 4th Ed., McGraw-Hill Book Company, 1986.
- [5] A. G. Phadke and J. S. Thorp, "Computer Relaying for Power Systems," Research Studies Press Ltd. ISBN 0 86380 074 2.
- [6] J. Z. Yang and C. W. Liu, "A Precise Calculation of Power System Frequency and Phasor," IEEE Transactions on Power Delivery, Vol. 15, No. 2, April 2000.
- [7] E. O. Schweitzer III and Daqing Hou, "Filtering For Protective Relays," 19<sup>th</sup> Annual Western Protective Relay Conference, Spokane, WA, October 20–22, 1992.
- [8] G. Benmouyal, "Removal of DC-Offset in Current Waveform Using Digital Mimic Filtering," IEEE Transactions on Power Delivery, Vol. 2, No. 2, pp. 621-30, April 1995.
- [9] A. G. Phadke et al., "Synchronized Sampling and Phasor Measurements for Relaying and Control," IEEE Transactions on Power Delivery, Vol. 9, No. 1, January 1994.
- [10] US Patent Number: 6,236,949. "Digital Sensor Apparatus and System for Protection, Control, and Management of Electricity Distribution Systems."
- [11] A. G. Phadke, J. S. Thorp, and M.G. Adamiak, "A New Measurement Technique for Tracking Voltage Phasors, Local System Frequency, and Rate of Change of Frequency," IEEE Transactions on Power Apparatus and Systems, Vol. PAS-102, No. 5, May 1983.
- [12] D. Hou, A. Guzman, and J. Roberts, "Innovative Solutions Improve Transmission Line Protection," 24<sup>th</sup> Annual Western Protective Relay Conference, Spokane, WA, October 21–23, 1997.
- [13] A. Guzman, J. B. Mooney, G. Benmouyal, N. Fischer, "Transmission Line Protection System for Increasing Power System Requirements," 55<sup>th</sup> Annual Conference for Protective Relay Engineers, College Station, Texas, April 8–11, 2002.
- [14] US Patent Number: 6,141,196. "Method and Apparatus for Compensation of Phasor Estimations."
- [15] E. O. Schweitzer III and J. Roberts, "Distance Relay Element Design," 19<sup>th</sup> Annual Western Protective Relay Conference, Spokane, Washington, October 20–22, 1992.
- [16] P. Bonanomi, "Phase Angle Measurements With Synchronized Clocks—Principle and Applications," IEEE Transactions on Power Apparatus and Systems, Vol. PAS-100, No. 12, December 1981.
- [17] G. Missout, J. Beland, G. Bedard, "Dynamic Measurement of the Absolute Voltage Angle on Long Transmission Lines," IEEE Transactions on Power Apparatus and Systems, Vol. PAS-100, No. 11, November 1981.

- [18] Ph. Denys, C. Counan, L. Hossenlopp, C. Holweck, "Measurement of Voltage Phase for the French Future Defence Plan Against Losses of Synchronism," IEEE Transactions on Power Delivery, Vol. 7, No. 1, January 1992.
- [19] J. S. Thorp, A. G. Phadke, S. H. Horowitz, M. M. Begovic, "Some Applications of Phasor Measurements to Adaptive Protection," IEEE Transactions on Power Systems, Vol. 3, No. 2, May 1988.
- [20] V. Centeno, J. De La Ree, A. G. Phadke, G. Mitchell, J. Murphy, R. Burnett, "Adaptive Out-of-Step Relaying Using Phasor Measurement Techniques," IEEE Computer Applications in Power, October 1993.
- [21] Y. Ohura, M. Suzuki, K. Yanagihashi, M. Yamaura, K. Omata, T. Nakamura, "A Predictive Out-of-Step Protection System Based on Observation of the Phase Difference Between Substations," IEEE Transactions on Power Delivery, Vol. 5, No. 4, November 1990.
- [22] A. G. Phadke, J. S. Thorp, K. J. Karimi, "State Estimation with Phasor Measurements," IEEE Transactions on Power Systems, Vol. PWRS-1, No. 1, February 1986.
- [23] Shweppe, F. C., Wildes, J., Rom, D. B., "Power System Static State Estimation I, II, III," IEEE Transactions on Power Apparatus and Systems, Vol. PAS-89, January 1970.
- [24] L. L. Grigsby, ed., Electric Power Engineering Handbook, CRC-IEEE Press, 2001.
- [25] IRIG Standard 200-95. "IRIG Standard Time Formats." Telecommunications Working Group, Inter-Range Instrumentation Group, Range Commanders Council.
- [26] IEEE Standard C37.111-1999. "IEEE Standard Common Format for Transient Data Exchange (COMTRADE) for Power Systems."
- [27] Schweitzer Engineering Laboratories, Inc., Application Guide AG2002.08, "Using SEL-421 Synchrophasor Measurements in Basic Applications," October 2002.
- [28] IEEE Standard C57.13-1993. "Standard Requirements for Instrument Transformers."

## APPENDIX

### Phasors as a Solution to a Differential Equation

Beginning with Equation 1, because the circuit is linear, the time current solution has the same form as the voltage waveform:

$$i(t) = I \cdot \cos(\omega \cdot t + \theta) \quad (\text{A.1})$$

Both the voltage and the current solution can be expressed in exponential form:

$$v(t) = V \left[ \frac{e^{j(\omega t + \phi)} + e^{-j(\omega t + \phi)}}{2} \right] \quad (\text{A.2})$$

and

$$i(t) = I \left[ \frac{e^{j(\omega t + \theta)} + e^{-j(\omega t + \theta)}}{2} \right] \quad (\text{A.3})$$

After substitution of Equations A.2 and A.3 into Equation 1, we obtain Equation A.4:

$$V \left[ \frac{e^{j(\omega t + \phi)} + e^{-j(\omega t + \phi)}}{2} \right] = R \cdot I \left[ \frac{e^{j(\omega t + \theta)} + e^{-j(\omega t + \theta)}}{2} \right] + L \frac{d \left\{ I \left[ \frac{e^{j(\omega t + \theta)} + e^{-j(\omega t + \theta)}}{2} \right] \right\}}{dt} \quad (\text{A.4})$$

By virtue of the principle of superposition applied to a linear network, this equation can be separated into two equations:

$$V \cdot e^{j(\omega t + \phi)} = R \cdot I \cdot e^{j(\omega t + \theta)} + L \frac{d[I \cdot e^{j(\omega t + \theta)}]}{dt} \quad (\text{A.5})$$

and

$$V \cdot e^{-j(\omega t + \phi)} = R \cdot I \cdot e^{-j(\omega t + \theta)} + L \frac{d[I \cdot e^{-j(\omega t + \theta)}]}{dt} \quad (\text{A.6})$$

From Equation A.5, we obtain the following after differentiation:

$$e^{j\omega t} V \cdot e^{j\phi} = e^{j\omega t} [R \cdot I \cdot e^{j\theta} + j\omega \cdot L \cdot I \cdot e^{j\theta}] \quad (\text{A.7})$$

The exponential term containing the time dimension can be cancelled because we have a single frequency. We are left with Equation A.8:

$$V \cdot e^{j\phi} = [R \cdot I \cdot e^{j\theta} + j\omega \cdot L \cdot I \cdot e^{j\theta}] \quad (\text{A.8})$$

Solve Equation A.8 to determine the magnitude and the phase angle of the current sinusoidal wave.

## BIOGRAPHIES

**Gabriel Benmouyal, P.E.** received his B.A.Sc. in Electrical Engineering and his M.A.Sc. in Control Engineering from Ecole Polytechnique, Université de Montréal, Canada in 1968 and 1970, respectively. In 1969, he joined Hydro-Québec as an Instrumentation And Control Specialist. He worked on different projects in the field of substation control systems and dispatching centers. In 1978, he joined IREQ, where his main field of activity was the application of microprocessors and digital techniques to substation and generating-station control and protection systems. In 1997, he joined Schweitzer Engineering Laboratories in the position of Research Engineer. He is a registered professional engineer in the Province of Québec, is an IEEE member, and has served on the Power System Relaying Committee since May 1989. He is the author or co-author of several papers in the field of signal processing and power networks protection. He holds one patent and has several patents pending.

**Dr. Edmund O. Schweitzer, III** is recognized as a pioneer in digital protection, and holds the grade of Fellow of the IEEE, a title bestowed on less than one percent of IEEE members. He has written dozens of technical papers in the areas of digital relay design and reliability and holds more than 20 patents pertaining to electric power system protection, metering, monitoring, and control. Dr. Schweitzer received his Bachelor's degree and his Master's in electrical engineering



from Purdue University, and his Ph.D. degree from Washington State University. He served on the electrical engineering faculties of Ohio University and Washington State University, and in 1982 he founded Schweitzer Engineering Laboratories to develop and manufacture digital protective relays and related products and services.

**Armando Guzmán, P.E.** received his BSEE degree with honors from Guadalajara Autonomous University (UAG), Mexico, in 1979. He received a diploma in Fiber-Optics Engineering from Monterrey Institute of Technology and Advanced Studies (ITESM), Mexico, in 1990. He served as Regional Supervisor of the Protection Department in the Western Transmission Region of Federal Electricity Commission (the electrical utility company of Mexico) for 13 years. He lectured at the Guadalajara Autonomous University (UAG) in power system protection. Since 1993, he has been with Schweitzer Engineering Laboratories, Inc., Pullman, Washington, where he is presently a Fellow Research Engineer. He holds several patents in power system protection. He is a registered professional engineer in Mexico, is a senior member of IEEE, and has authored and co-authored several technical papers.